

Article

Implementation of Digital Twin for Increasing Efficiency of Renewable Energy Sources

Milan Belik ^{1,*} and Olena Rubanenko ^{1,2,3,4} 

¹ Department of Electrical Power Engineering, Faculty of Electrical Engineering, University of West Bohemia, 30614 Pilsen, Czech Republic; rubanenk@fel.zcu.cz

² Research and Innovation Center for Electrical Engineering (RICE), Faculty of Electrical Engineering, University of West Bohemia, 30614 Pilsen, Czech Republic

³ Department of Power Plants and System, Vinnitsya National Technical University, 21000 Vinnitsya, Ukraine

⁴ Department of Wind Power, Institute of Renewable Energy, 02094 Kyiv, Ukraine

* Correspondence: belik4@fel.zcu.cz

Abstract: This paper presents an analysis of the instability of the electricity generation of renewable energy sources (RESs), specifically Digital Twins of RESs. The first part deals with the analysis of RES electricity generation around the world and Ukraine. The following chapter describes features of functioning power grids in modern conditions in Ukraine and ways to ensure the balance reliability in the power system for conditions of high-grade RES integration. The rapid increase in electricity generation RESs causes control problems of distributed power supply in the power grid. A mathematical model of the parameter controls in normal mode electric power systems for conditions with high integration of RESs is proposed in the second part. The study investigates components of the optimality criterion at the control of normal mode parameters of the electric power system with RESs. In general, digital transformation helps decarbonize the energy supply, decrease dependency on fossil fuels, and integrate renewables into power systems. A model Digital Twin (DT) of a photovoltaic system, or an exact 3D visualization, analyzing the accumulator system depending on load and generation, are presented. The problems of Digital Twin are very widely discussed, but many papers and studies are general without any practical implementations. The main part of this paper focuses on research and deals with daily electricity generation from different kinds of RESs, namely mini-hydropower stations, photovoltaic power stations, and wind power stations. Measured data of electricity generation from photovoltaic power plants, wind power plants, and mini-hydropower plants and obtained meteorological factors were used for the calculation of Spearman's, Kendall's, and Pearson's correlation rank coefficients. The main contribution of this research is to determine the main metrological factors for each kind of studied RES. In the future, it will help to decide the task of forecasting power generation more presciently. Additionally, the presented model of DT RESs allows the installation and operation of grids with higher efficiency, because it can help to predict all influences, from shading up to the optimization of the battery storage system.

Keywords: digital twin; renewable energy sources; photovoltaic power plant; wind power plant; small hydropower plant; instability; criteria correlation Spearman



Citation: Belik, M.; Rubanenko, O. Implementation of Digital Twin for Increasing Efficiency of Renewable Energy Sources. *Energies* **2023**, *16*, 4787. <https://doi.org/10.3390/en16124787>

Academic Editors: Mariano Giuseppe Ippolito and Abu-Siada Ahmed

Received: 10 May 2023

Revised: 1 June 2023

Accepted: 13 June 2023

Published: 18 June 2023



Copyright: © 2023 by the authors. Licensee MDPI, Basel, Switzerland. This article is an open access article distributed under the terms and conditions of the Creative Commons Attribution (CC BY) license (<https://creativecommons.org/licenses/by/4.0/>).

1. Introduction

Integration of renewable energy sources (RESs) into power systems (PSs) is a strong trend impacting many subjects in local specifics of particular countries. The task of decreasing CO₂ emissions is a worldwide challenge [1]. Renewable energy source (RES)-based electrification is an important step for changing the ecological situation in the world [2,3]. Detailed art analyses allow us to highlight four main renewable sources: wind renewable energy, solar renewable energy, hydro renewable energy, and bioenergy (see Figure 1) [2,4,5].

Replacement of conventional electric power plants using fossil fuels with renewable energy sources can help to answer this challenge [1]. According to IRENA [6], there is currently a rapid increase in installed capacity and RES electricity generation in the world, Europe and Ukraine as well. In Ukraine, the most popular RESs are photovoltaic power stations (PPSs), wind power stations (WPSs), and small and micro hydropower stations (HPSs).

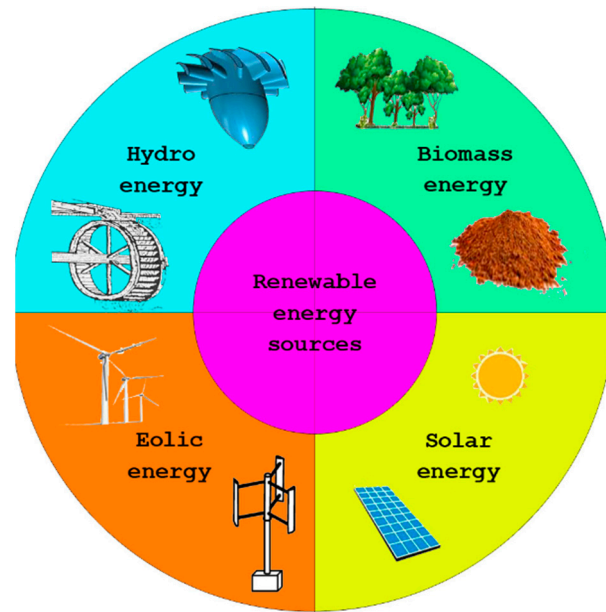


Figure 1. Potential RESs.

It is evident that the actual task is improving the methodology of control, management, and programming of DT photovoltaic systems, which provides an abstraction of the entire system as a distributed database. Experiments will implement on a simulation platform in real time. In contrast, it is planned to develop a real-life simulation model for researching the process of implementing DT technologies in the power balancing of the electric system of microgrids with RESs based on the theory of similarity and neuro-fuzzy modeling while taking into account the technical conditions of RESs.

The research work planned studies the digitalization of Renewable Energy Sources (RESs), creating an exact Digital Twin (DT) with the aim of supporting the balancing of the power grid and increasing the flexibility of the energy system, made possible through dispatchable renewable energy sources. An essential part of the network systems needs total reconstruction, renewal, and modernization. The objective is to study and increase the potential and performance of renewable energy sources with the usage of DT.

In accordance with the formed goal and objectives of the scientific work, it is assumed that the analysis and summary of the actually collected information will be carried out. On the basis of summarizing the results and the results of the analysis of information reports on the subject of the project, this study planned to conduct a marketing study and provide proposals to customers. Potential practical benefits from the project apply to customers and companies engaged in the design, installation, and operation of solar power plants, as well as to the Scientific and Design Center for the Development of the Unified Energy System of Ukraine at NEC “Ukrenergo” for the improvement in regulatory documents regulating the operation of renewable energy sources in electrical networks of energy systems.

RESs play a significant role in the energy transition, meaning more than 50% of the primary energy supply and almost 100% of electricity production [4]. IRENA’s quantification of renewable energy focusing on the power market globally shows that existing goals aim to increase the total renewable energy capacity up to 5.4 TW by the end of this decade. This is exactly half of the 10.8 TW needed to reach IRENA’s 1.5 °C scenario [5]. Figure 2 shows the targets to be achieved by the installation of PV systems, at onshore as well as

offshore wind parks, by 2030. The large usage of PV and wind energy is expected, which gives a significant decrease in the cost of these technologies. The change has reached 88%, 68%, and 60% in the levelized cost of energy (LCOE) between 2010 and 2021 [6].

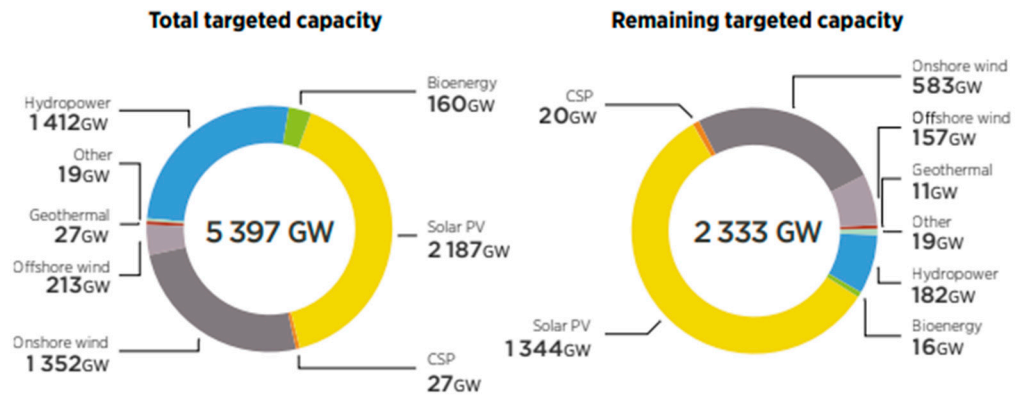


Figure 2. Quantified targets by RES technology around the world [6].

The dynamics of changes in RES electricity generation in Ukraine differ from the rest of the world because of the present war conditions, so they need to be investigated in more detail. Data from IRENA for Ukraine RES generation are presented in Figures 3 and 4. In IRENA online resources, in terms of RES potential, the local solar power potential in Ukraine can be classified into seven groups. Every group represents one range of annual PV production per nominal unit of installed capacity (kWh/kWp/yr). The presented chart shows the percentage of the selected country’s applicable area in every class and the total distribution of applicable area inside all classes as a numerical comparison.

Potential wind power density (W/m^2) for onshore wind farms and installations is presented in these particular classes used by NREL. The value is measured at the height of 100 m above the terrain. The chart also compares the distribution of the country’s free area in each of these classes and matches it to the full sum of all wind resources. Locations in the third group or higher are considered to be good wind resources and thus applicable for usage of this source. Net primary production (NPP) of biomass is the full amount of carbon stored inside all plants and accumulated as a biomass source every year. This number is the basic measure of biomass production effectiveness. The presented chart shows the average NPP for the model country (tC/ha/yr). This value is compared to the average NPP of 3–4 t of carbon for the entire planet [5].

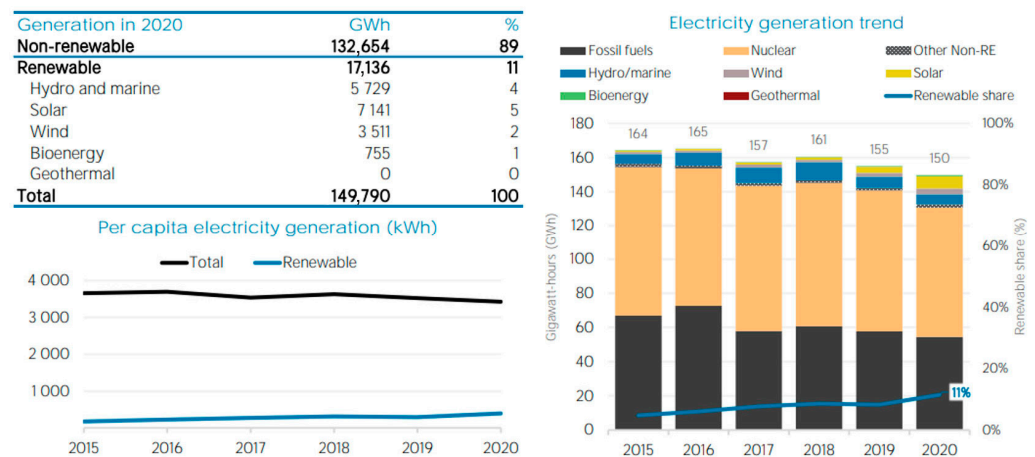


Figure 3. Electricity generation in Ukraine, according to IRENA 2021 reports.



Figure 4. Distribution of solar and wind potential in Ukraine [6].

One of the ways to increase the efficiency of RESs in the power grid is the usage of Digital Twin for operation [7,8].

2. Digital Twin for RESs

Digital transformation helps to decarbonize the energy supply, decrease dependency on fossil fuels, and integrate renewables in PSs while increasing their resilience [9]. RESs can also be used for the power and heat supply of shelter cities. A shelter city is a community of citizens (refugees) who lost their homes in war conditions. The building of shelter cities generates problems in existing PSs and also impacts the power quality in the affected power grid. The development of digital solutions and Digital Twins (DT) also makes this application more reliable and affordable. The global DT market size is expected to reach \$41.77 billion in 2026 [10]. DT implementation developed and adopted for war or post-war PS conditions can make shelter city prosumers, and thus another benefit for the PS (Figure 5). RES DTs manage their day-to-day operations and optimize performance to increase efficiency and speed up the reaching of the EU target that the usage of electricity produced by renewables must grow to 50% by 2030.

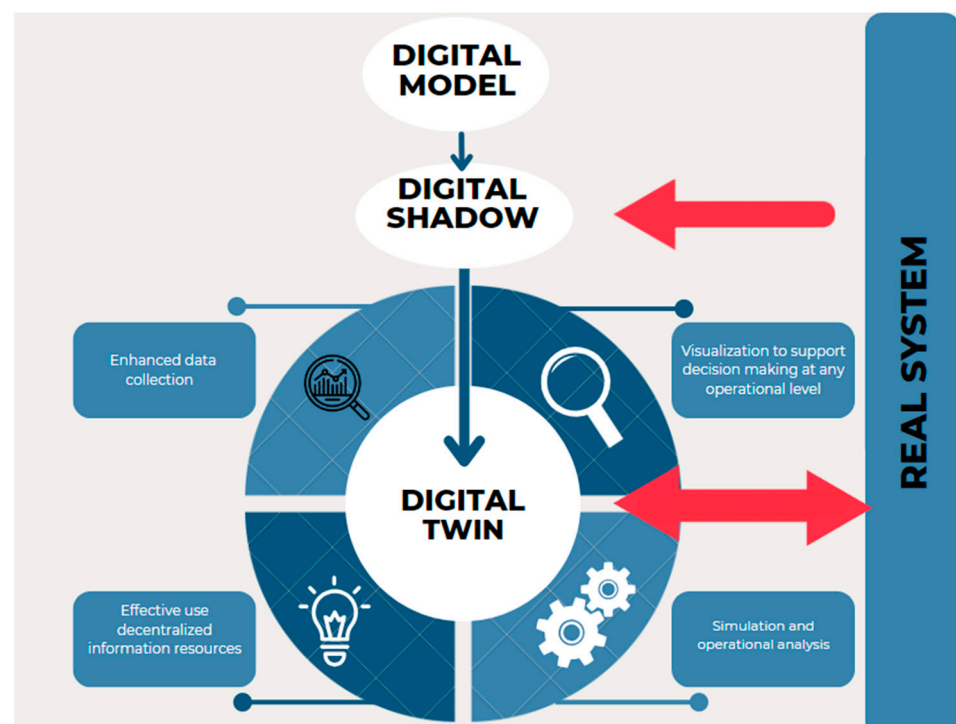


Figure 5. Flowchart for implementation of DT in operation of DRESS.

Several research studies [11–14] concentrated on practical issues and presented a case study: an assessment of a PV inverter integration to a highly distributed renewable energy source (DRES)-penetrated microgrid and described DT of RES equipment. The process of implementing DT in RESs is presented in the flowchart in Figure 5.

The CORDIS Results Pack report presented EU-funded projects developing digital solutions (including DT) to build a secure and diversified energy supply to improve RES efficiency and resilience, reduce emissions, and provide citizens with innovative energy services. Vision 2030 on Market Design and System Operation presents ENTSO-E [11] identified drivers for power systems in the next 10 years: the rise of renewables (green deal), the drive for electrification, the increase in decentralized resources, and digitalization.

The INTERFACE project develops an interface between transmission and distribution system operators and their customers to allow seamless integration and efficient use of RESs in the grid [14]. The FLEXIGRID project finds solutions that will protect the security and reliability of the electricity grid as it incorporates growing amounts of RESs [15].

The TwinERGY project introduced a first-of-a-kind DT framework that will incorporate the required intelligence for optimizing energy demand and responsible RES usage. TwinERGY further reinforces and catalyzes collaborative advancements in research, innovation, regulation, and market issues around Demand Response, RES Integration, and Consumer Engagement [16].

Furthermore, these DTs will provide the basis for new market structures and will allow wider use of distributed RESs. In the heart of digital transformation lies the process of assigning real, physical embodiments and digital identities, also called Digital Twins. DT is then used to support processes of design, development, monitoring, and targeting interoperability between reality and digital representations of any asset. The level of correspondence between the real object and its DT is critical, as it impacts the accuracy of the information available through the DT and the reliability of any decision based upon it. The PV industry progresses fast on the path of digital transformation. Basic singular DTs are already in use across the lifecycle of PV assets, starting from design through monitoring, all way to decommissioning and dismantling [17]. The current state of research shows the relevance of the proposed topic and the need to develop methods and recommendations for controlling RESs with DT usage. These DTs can also help optimize the power supply of the shelter city (Figure 6).

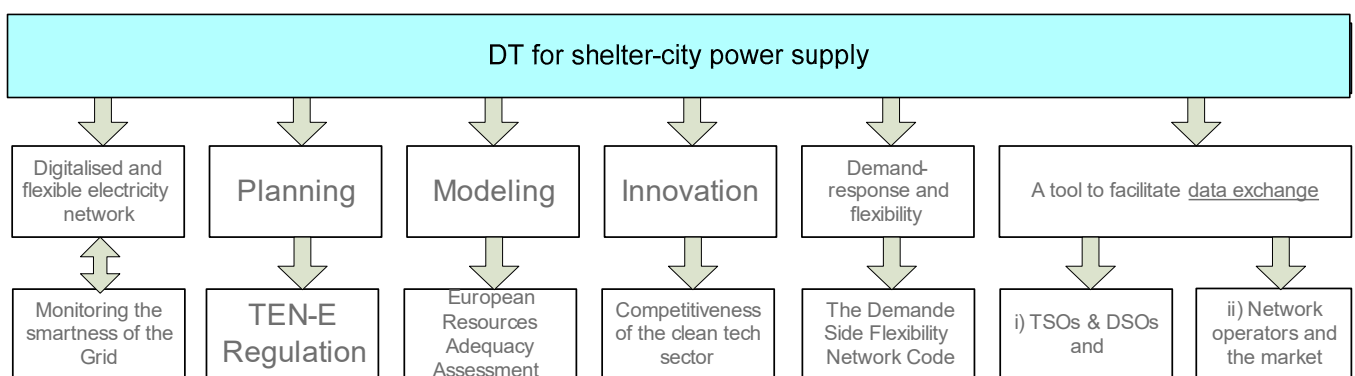


Figure 6. DTs for shelter city and RESs.

3. Integrated DTs for RESs in TSOs and DSOs

The main keys of DT technologies for integrated energy systems are presented in Table 1 [18].

Table 1. Key technologies of integrated hybrid energy system.

Technology	Description
Multifunctional synergy	This determines the ideal energy resource distribution in the affected region. It arises from the current situation in economy and resource potential.
Energy conversion	This means converting the primary energy into secondary energy. Energy storage and energy transportation costs are to be significantly reduced.
Intelligent	Intelligent (smart) monitoring is the background of this principle. It is usually combined with the cooperation between edge intelligence, sophisticated data analysis, and fast processing.
Energy cascade utilization	The reduction in energy consumption follows smart energy usage. Depending on required quality and energy usage, all particular steps are sequentially repeated.

Integrated DTs in power systems have weaknesses, and there is a push to find new approaches for the physical implementation of DTs in TSOs for RESs:

1. Integrated modeling of multi-physics information hybrid systems, which means the DT of any coupled energy system. This can contain coupling modeling of the considered complex energy lines, or associative modeling of the doublet information–physical object. Reducing and simplifying the mentioned physics–information twin leads to the hybrid model;
2. A data-driven understanding of complex link features is essential for a comprehensive energy system that is difficult to survey directly. This is built on mechanism analysis and calculation and utilizes dynamic optimization of the unsurveyable object’s model. It also takes into account real measured information;
3. A stable solution for the multivariate heterogeneous model means focusing on the solution complexity defined through particular components of the DT hybrid model. The basic means is the creation of a consistent solution framework that is fully compatible with all other model features, including the communication interfaces and real interactions of the proposed hybrid model. The next step is the multi-scale collaborative solution. Both the hybrid and heterogeneous models must be in correlation with the parallel stability solution of twin real–digital objects as well;
4. Multi-scene applications and feedback integrating realistic measurements represent real holographic mirroring capacity as well. Both objects are able to have digital–reality interaction. These features of the proposed DT are applied, generally including also the virtual–real information linking mechanism that is necessary for mirroring operated in real time. Next, the prospective simulation of the running trajectory includes the calculation of the model’s uncertainty, and finally, the self-evolution of DTs can be built on the operational data feedback mechanism.

4. Features of DT Usage for Optimal Control of Distributed Power Systems with High-Penetration RESs

Some types of tasks need to be decided to implement DT RESs, such as dynamic systems with optimal conditions of RES operation management. DT RESs are described by long-term- short-term prediction, planning, maintenance, and operational control in real-time mode. The main task of DT RESs is a comparison of different types of control (operational and automatic). The economic efficiency implementation of the DT solution strongly depends on how well the DT RES task is defined. The strong issue during the

implementation of DT for RESs is the discovery of reliable virtual models (mathematical models) that consider the dynamics of RES generation and load power grid.

The feature of the use of existing optimization methods is the mathematical formalization of the processes that are optimized for presentation with the usage of expensive software. However, in the mathematical modeling of systems that have a complex temporal and spatial hierarchical structure, there are significant complications. The main ones are the multicriteria of control, as well as the distribution over a large area and the need to combine in time the task of short-term planning, operational (dispatching), and automatic control.

In general, the existing relationships between the parameters of the control process and the parameters of the elements of the system in which this process takes place can be presented as follows [19]:

$$y(u) = \sum_{i=1}^{m_1} a_i \prod_{j=1}^n u_j^{\alpha_{ji}} \quad (1)$$

where $y(u)$ is a generalized technical and economic indicator; a_i , α_{ji} are constant coefficients determined by the properties of the system; u_j is the variable system parameters; m_1 is the number of members of the function; and n is the number of variables.

In the optimization problems under consideration, the exponent y is the criterion of optimality, and Expression (1) is the objective function. When solving optimal control problems, it is necessary to compare options and choose the best one according to a certain criterion. A comparison of options should be made with the basic values y_b and u_b . Any variant of the state of the system can be expressed through these quantities. This can be performed in this way.

Let us mark

$$y = y_* \cdot y_b, \quad u_j = u_{j*} \cdot u_{jb} \quad (2)$$

where $y_* = y/y_b$ and $u_{j*} = u_j/u_{jb}$ are the relative values of the parameters.

Substituting (2) into (1), we obtain

$$y_* \cdot y_b = \sum_{i=1}^{m_1} a_i \prod_{j=1}^n u_{j*}^{\alpha_{ji}} u_{jb}^{\alpha_{ji}} \quad (3)$$

Performing identical transformations and introducing a replacement,

$$\pi_{ib} = \frac{a_i \prod_{j=1}^n u_{jb}^{\alpha_{ji}}}{y_b} \quad (4)$$

We obtain the criterion form of the problem record:

$$y_* = \sum_{i=1}^{m_1} \pi_{ib} \prod_{j=1}^n u_{j*}^{\alpha_{ji}} \quad (5)$$

Note that for the basic variant, when $y = y_b$, the criterion Equation (5) will take the following form

$$1 = \pi_1 + \pi_2 + \dots + \pi_{m1} \quad (6)$$

In the last equation, the similarity criteria are normalized to 1. They indicate the relative share of each member of the function (each component) in the criterion of optimality.

Considering the criterion Equation (5), it is easy to see that it allows us to investigate the effect of deviation of any of the variables u_j from its optimal value on the value of the optimality criterion, to investigate the optimal solution on the sensitivity. Obviously, it is most convenient to do this in relative units. If, by condition, the sensitivity of the optimal solution is to be obtained in named units, then such a possibility exists. Expression (2) can be used to recalculate deviations or variations. Obviously, it is first necessary to determine the optimal (basic) values of the parameters of the studied system. To do this,

you can use any of the known optimization methods. However, it is best, in this case, to use criterion programming, because in it, the similarity criteria are variables that are optimized [19,20]. In [19], a technique was developed in which the transition from double variables of criterion programming (similarity criteria) to variables of a direct problem is provided.

The experience of implementing optimization programs in the practice of operational control shows that to achieve noticeable efficiency, it is necessary to constantly adjust the parameters of the RES. The control and correction of states are based on a comparison of the current and optimal value of the optimality criterion, which is the main core of the DT,

$$\Delta F = F_{cur} - F_o \quad (7)$$

where ΔF is the value that characterizes the difference of the optimality criterion between its current value F_{cur} and the optimal F_o in a certain period of time to control the conditions of the system.

It is obvious that the complete coincidence of F_{cur} and F_o in real technical systems for various reasons is impractical and sometimes impossible, for example, due to the discreteness of the change in regulatory parameters. To achieve equality $F_{cur} = F_o$ in dynamic systems, such as power grids, requires a high intensity of DT, which leads to the rapid use of their technical resources, reduced reliability, and consequently, to failures and losses, sometimes commensurate and even greater than technical-economic effects, which are achieved as a result of optimization. The general approach to solving this problem is the analysis of the sensitivity of the criterion of optimality and the establishment of a reasonable zone of insensitivity, in the middle of which all variants of the system are equal economically.

Paper [19] shows the fundamental possibility of using similarity theory and modeling in relation to the sensitivity problems of control systems. It is necessary to research and develop appropriate methods and tools, as well as to determine the best ways to use them.

An important step in the analysis and evaluation of the sensitivity of optimal solutions, which largely determine the efficiency of the system as a whole, is to create an adequate mathematical model [21]. In this regard, it is necessary to develop mathematical models that allow us to more effectively solve the problems of sensitivity analysis of optimal solutions for controlling the conditions of dynamic systems. They should allow analyzing and, on the basis of the results of the analysis, interpreting the received optimum of the model on an optimum of the real investigated scheme. In the criterion models for this purpose, it is necessary to match the accuracy of the definition of similarity criteria with the accuracy of the initial information and the practical implementation of optimal solutions.

The individual elements of the systems considered here are interconnected in such a way that their aggregate properties are described by graphs or matrices. The relationships of the parameters of the vertices and edges of the graph in the mathematical models used in optimal control are reduced to a quadratic form. Each member of this form is a square of one of the variables or the product of two different variables. In matrix form, it is written in the form

$$f(x) = \mathbf{x}_t \mathbf{Q} \mathbf{x} \quad (8)$$

where \mathbf{Q} is a symmetric matrix, the rank of which is the rank of the form $f(x)$.

In mathematical models of optimization problems during the formation of the objective function as a function of the parameters of the vertices of the graph, it is necessary to represent the quadratic form in the canonical form [19], which is when it contains only the sum of terms with the squares of variables. Accordingly, it is necessary to convert the matrix \mathbf{Q} to a diagonal, which is always possible with orthogonal transformation. In this case, the vector \mathbf{x} is transformed, where \mathbf{S} is the similarity transformation matrix, such that

$$\tilde{\mathbf{Q}} = \mathbf{S}_t \mathbf{Q} \mathbf{S} \quad (9)$$

where \tilde{Q} is the diagonal matrix, on the main diagonal of which are the eigenvalues of the matrix Q ; S is the matrix sensitivity.

Thus, it is necessary to develop a method for assessing the sensitivity of the mathematical model of optimal control with eigenvalues.

The quality of optimal control significantly depends on the validity of the selected insensitivity zone of the optimality criterion and the definition of the corresponding insensitivity zones of the parameters that are regulated. Since the operating conditions in the systems under consideration are constantly changing, it is necessary to adapt the SAC to them. To this end, it is necessary to develop an algorithm and a program for determining the boundaries of the region of insensitivity (optimality) of the components of the state control vector of systems in which the mismatch of current and optimal states is characterized by large losses.

In [21–23], the laws of state control of a system with a quadratic optimality criterion are obtained. However, they do not take into account the influence of the accuracy of parameter determination on the accuracy of calculating similarity criteria as feedback coefficients of the control laws of the species. For control, errors in determining the similarity criteria lead to the incomplete correspondence of the optimal conditions of the mathematical model of the system and the real system. It is necessary to develop methods, algorithms, and programs for DT RESs for the formation and practical implementation of the laws of optimal control for the conditions of a dynamic system, taking into account the sensitivity and thus deviating from the errors of the initial information and computational inaccuracies. With developed methods, algorithms, and programs, DT can help involve imbalanced power systems with high-penetration RESs.

5. The Imbalance in Electric Power Systems with RESs in Case of Ukraine

The imbalance in electric power systems is observed (not just) in Ukraine. This phenomenon is caused by the rapidly increasing generation of PPPs and WPPs. Insufficient maneuverability and power capacity for balancing can also lead to an imbalance in the whole system.

This situation in the electric networks against the background of the trends of the annual increase in installed capacity and electricity generation by renewable energy sources (RESs) poses new challenges and issues.

Nowadays, in Ukraine, there are particularly pressing issues of imbalanced electrical networks. Since 1 January 2021, the standard for the financial responsibility for the imbalance of the electrical power in the electrical system has been accepted. Energy supply companies, which are generating power via RESs, will pay financial taxes for power imbalances. In these conditions, the problem of the analysis of electricity generation RES instability at the control of parameters of electric network modes is actualized [24]. Forecasting electricity generation with minimal error to minimize possible compensation for inaccurate forecast data is necessary for PPS, WPS, and mini-HPS owners. Forecasting and usage of DTs are becoming significant tools for the cost-effective integration of RES systems such as wind, solar, and hydro into microgrids, local and regional distribution grids, and national transmission systems.

It should also be noted that, even due to the large number of software packages and algorithms that allow the formation of forecast data, the issue of reliable and accurate forecasting still requires new deep studies and research projects, because the constant change in climate and thus local weather significantly complicates the forecasting process. The forecasting process precedes the process of analyzing the instability of RES generation, namely the identification of the most influential meteorological factors, so this article is devoted to the analysis of the instability of RES generation in the control of electrical networks.

It should also be noted that, even due to a large number of software and algorithms that allow the formation of forecast data, the issue of reliable and accurate forecasting still requires careful study and research, because the constant change in weather significantly complicates the forecasting process.

The forecasting process precedes the process of analyzing the instability of RES generation, namely the identification of the most influential meteorological factors, so this article is devoted to the analysis of the instability of RES generation in the control of electrical networks. So, features of functioning power grids in modern conditions are shown in Figure 7 and were created with the analysis papers taken into account [24–26].

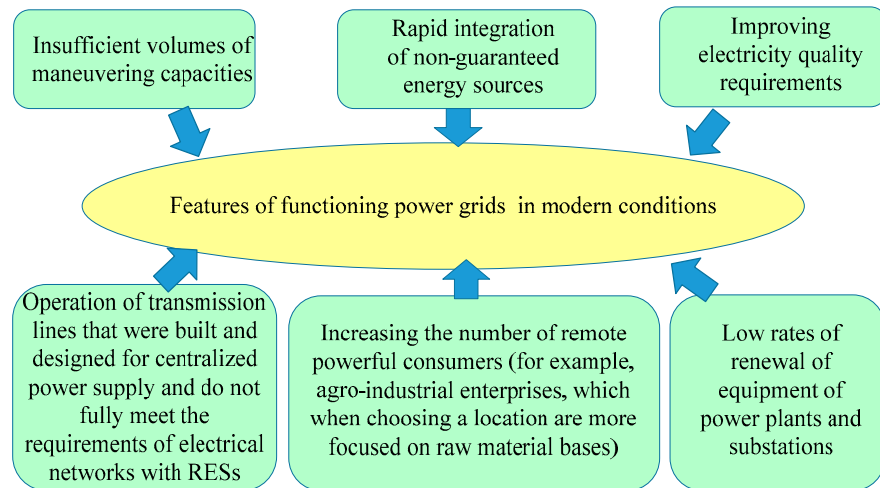


Figure 7. Features of functioning power grids in modern conditions in Ukraine.

Ensuring the balance and, thus, better reliability in the power system in conditions of RES integration is possible with the means and approaches that are presented in Figure 8 [21,22,27].

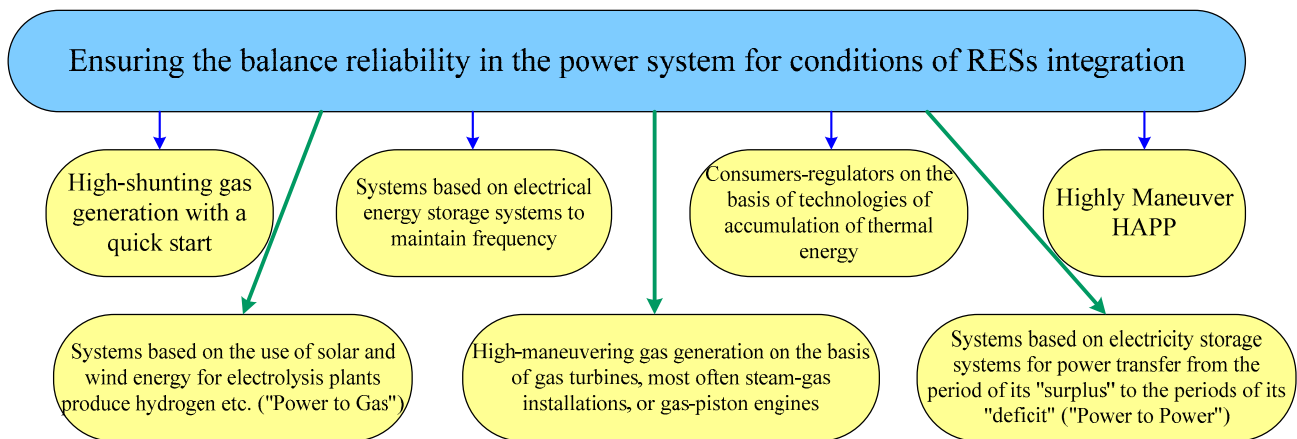


Figure 8. Ways of ensuring balance reliability in the power system in conditions of high-grade RES integration.

6. The Control of the Parameters of Normal Mode Electric Power System for Conditions with High-Level Integration of RESs

More details about this are written in the paper [28–31]. The optimal control task of the parameters of the electric power system in its normal mode can be presented by the expression [32]: minimize the control function

$$F(u) = \int_{t_0}^{t_k} [\mathbf{x}_t(t)\mathbf{H}\mathbf{x}(t) + \mathbf{u}_t(t)\mathbf{L}\mathbf{u}(t)]dt \tag{10}$$

in the set of states of the electric power system:

$$\frac{dx}{dt} = \mathbf{Ax}(t) + \mathbf{Bu}(t); \mathbf{x}(t_0) = \mathbf{x}_0; \tag{11}$$

$$\mathbf{y}(t) = \mathbf{Cx}(t) + \mathbf{Du}(t); \tag{12}$$

where $\mathbf{x}(t)$ is the vector of state; $\mathbf{y}(t)$ is observation, $\mathbf{u}(t)$ is the control vector; \mathbf{A} , \mathbf{B} , \mathbf{C} , \mathbf{D} , \mathbf{H} , and \mathbf{L} are matrixes of constant indexes, which are characterized by electric power system parameters and have physical content; t_0 and t_k are the beginning and the end of the time interval at which the control function to minimize (during 15 min for dispatch control of the electric power system); and \mathbf{x}_0 is the start point of the state vector.

In this model:

$$\mathbf{x}(t) = \begin{bmatrix} \dot{\mathbf{J}}(t) \\ \dot{\mathbf{U}}_{\Delta}(t) \\ U_b \end{bmatrix}; \mathbf{y}(t) = \begin{bmatrix} \dot{\mathbf{S}}_b(t) \\ \dot{\mathbf{U}}_b(t) \\ U_b \end{bmatrix}; \mathbf{u}(t) = \begin{bmatrix} \mathbf{k}(t) \\ \mathbf{Q}_{RPS}(t) \\ \mathbf{S}_{RES}(t) \\ \mathbf{P}_{SE}(t) \end{bmatrix}; \tag{13}$$

where $\dot{\mathbf{J}}(t) = \hat{\mathbf{U}}_d^{-1}(t)\hat{\mathbf{S}}(t)$ is the vector of currents in nodes; $\hat{\mathbf{U}}_d(t)$ is the diagonal matrix of node voltage; $\hat{\mathbf{S}}(t) = \mathbf{P} + j\mathbf{Q}$ is the vector of powers in nodes; $\dot{\mathbf{U}}_{\Delta}(t)$ is the vector of the voltages of the nodes relatively basic; U_b is the voltage of the base node; $\dot{\mathbf{U}}(t)$ is the vector of node voltages; $\dot{\mathbf{S}}_b(t) = \mathbf{P}_b + j\mathbf{Q}_b$ and $\dot{\mathbf{I}}_b(t)$ are vectors of powers and currents in the EPS branches where tele-measurements are; and $\mathbf{k}(t)$, $\mathbf{Q}_{RPS}(t)$, $\mathbf{S}_{RES}(t)$, and $\mathbf{P}_{SE}(t)$ are vectors of transformation coefficients, loads of reactive power sources, power of RESs, and power of storage energy systems [25]. The state of the electric power system is defined in Equation (2), and its solution respects the initial conditions $\mathbf{x}(t_0) = \mathbf{x}_0$.

Components of the optimality criterion at the control of normal mode parameters of electric power systems with RESs are shown in Figure 9 [24,26–30]. Following the investigation components of the optimality criterion for control in electric power systems, the next step of the research is to study the influence of meteorological factors on the generation of RESs [31–33].

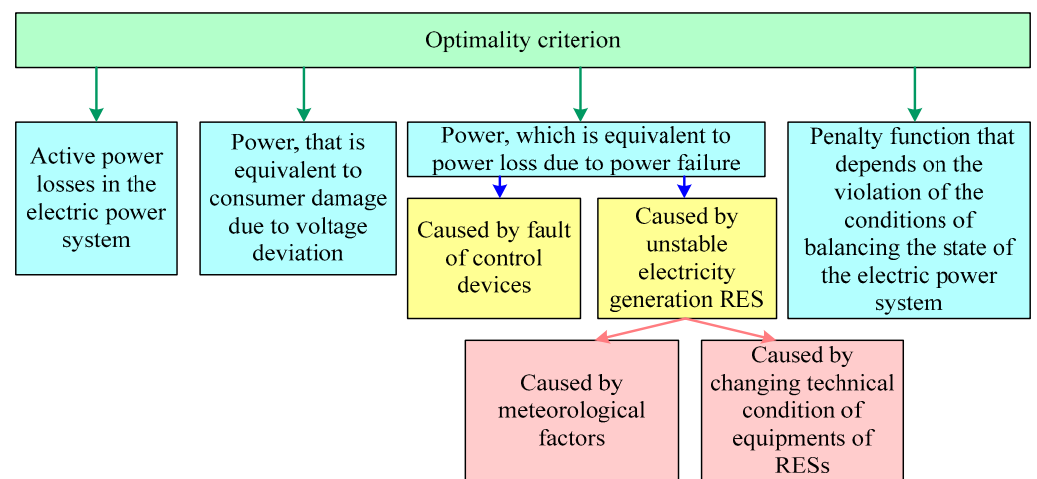


Figure 9. The optimality criterion.

7. Assessment of the Sensitivity of the Optimality Criteria

Usually, during the synthesis of optimal programs and control laws, a priori information on the dynamic characteristics of the object, possible external perturbing influences, initial conditions for certain parts of the control process, etc., are used. However, the actual characteristics of the systems differ from those expected. As a result, the design control may be suboptimal. In addition, the control itself, as a result of errors in measuring elements, computing, and actuators, is usually different from the calculation. This can also lead to a

violation of the conditions of optimality. To assess the influence of these factors on the value of the criterion of optimality, it is possible to use the apparatus of sensitivity theory [27].

The function that characterizes the quality of the optimality system and is denoted in paragraph 5 as $F(x, u)$ is written as follows:

$$F = F[x(t, \varepsilon_1, \dots, \varepsilon_m, u_1, \dots, u_n), \varepsilon_1, \dots, \varepsilon_m, u_1, \dots, u_n, T], \quad (14)$$

where ε_i is a parameter that can have different physical values (it can characterize both the eigenvalues of the system under study and the external actions acting on it), and T is time intervals that characterize the period of discreteness of control actions.

It is assumed that the problem of finding the optimal control solution is reduced to the problem of the conditional extreme of the function of many variables. The optimal value of the function at the calculated values of the parameters $\varepsilon_1, \dots, \varepsilon_m$ is written in the form

$$F_0 = F[x(t, \varepsilon_{10}, \dots, \varepsilon_{m0}, u_{10}, \dots, u_{n0}), \varepsilon_{10}, \dots, \varepsilon_{m0}, u_{10}, \dots, u_{n0}, T]. \quad (15)$$

Let the real values of the parameters ε_i and u_i differ from those calculated for the small quantities $\Delta\varepsilon_i$ and Δu_i . Assume that the minimum of the function F is reached within the allowable range of control parameters. Therefore, the partial derivatives characterizing the sensitivity of the function to changes $\frac{\partial F}{\partial u_i}$ in the parameters u_i are zero.

Then, decomposing (15) into a Taylor series and ignoring the terms above the first order with respect to $\Delta\varepsilon_i$ and Δu_i obtains

$$\Delta F = \sum_{i=1}^m \frac{\partial F}{\partial x} \cdot \frac{\partial x}{\partial \varepsilon_i} \Delta \varepsilon_i + \sum_{i=1}^m \frac{\partial F}{\partial \varepsilon_i} \Delta \varepsilon_i. \quad (16)$$

From relation (10), the obtained sensitivity of the considered function (14) to changes in the parameters is estimated using the expression

$$\delta_i^F = \frac{\partial F}{\partial x} \cdot \frac{\partial x}{\partial \varepsilon_i} + \frac{\partial F}{\partial \varepsilon_i}$$

This paper solves the problem in which the function of the form is used as an indicator of optimality, as follows:

$$F = \int_{t_0}^{T(\varepsilon)} f(x, u, t, \varepsilon) dt \quad (17)$$

Time T can be set or be a function of ε in advance. In the latter case, the moment T is determined by a scalar condition

$$\Omega[x(T), T, \varepsilon] = 0. \quad (18)$$

It is obvious that the time T is a function of the parameter ε .

The sensitivity function of the indicator (12) has the following form:

$$\frac{\partial F}{\partial \varepsilon} = f[x(T), u(T), T, \varepsilon] \frac{dT}{d\varepsilon} + \int_0^T \left[\frac{\partial f}{\partial x} \cdot \frac{\partial x}{\partial \varepsilon} + \frac{\partial f}{\partial u} \cdot \frac{\partial u}{\partial \varepsilon} + \frac{\partial f}{\partial \varepsilon} \right] dt$$

In the latter expression, the derivative $\frac{dT}{d\varepsilon}$ is determined by relation (18):

$$\frac{dT}{d\varepsilon} = - \frac{\frac{\partial \Omega}{\partial x} \cdot \frac{\partial x}{\partial \varepsilon} + \frac{\partial \Omega}{\partial \varepsilon}}{\frac{\partial \Omega}{\partial x} \cdot \frac{\partial x}{\partial T} + \frac{\partial \Omega}{\partial T}}$$

or

$$\frac{\partial T}{\partial \varepsilon} = \frac{\frac{\partial \Omega(T)}{\partial x} \delta(T) + \frac{\partial \Omega(T)}{\partial \varepsilon}}{\frac{\partial \Omega(T)}{\partial x} f[x(T), u(T), T, \varepsilon] + \frac{\partial \Omega(T)}{\partial T}} \quad (19)$$

where $\delta(T)$ is the sensitivity function of the solution at $t = T$, and $f[x(T), T, \varepsilon]$ is the right part of the differential equation of the system at $t = T$.

In principle, the function of the parameter ε can be the lower limit of integration in the function t_0 (19):

$$t = t_0(\varepsilon).$$

In this case, t_0 is determined by a scalar equation

$$\Omega_1[x(t_0), t_0(\varepsilon), \varepsilon] = 0. \quad (20)$$

The sensitivity function of the quality criterion (20), in the case when t_0 is variable, is determined by the expression

$$\begin{aligned} \frac{\partial F}{\partial \varepsilon} = & f[x(T), u(T), T, \varepsilon] \frac{dT}{d\varepsilon} - f[x(t_0), u(t_0), t_0, \varepsilon] \frac{\partial t_0}{\partial \varepsilon} + \\ & + \int_0^T \left[\frac{\partial f}{\partial x} \cdot \frac{\partial x}{\partial \varepsilon} + \frac{\partial f}{\partial u} \cdot \frac{\partial u}{\partial \varepsilon} + \frac{\partial f}{\partial \varepsilon} \right] dt \end{aligned} \quad (21)$$

In (21), the derivative $\frac{dT}{d\varepsilon}$ is found by Formula (19), and the derivative $\frac{\partial t_0}{\partial \varepsilon}$ is found by the following formula:

$$\frac{\partial t_0}{\partial \varepsilon} = - \frac{\frac{\partial \Omega(t_0)}{\partial x} \delta(t_0) + \frac{\partial \Omega(t_0)}{\partial \varepsilon}}{\frac{\partial \Omega(t_0)}{\partial x} f[x_0, u_0, t_0, \varepsilon] + \frac{\partial \Omega(t_0)}{\partial t_0}} \quad (22)$$

With the help of sensitivity functions, it is possible to estimate the influence of inaccuracies of the initial information on parameters of an invariable part of the system (object, executing devices, and sensors); disturbing effects; and initial conditions on the values of the parameters that determine the optimality of control.

Consider an example function

$$F = F(\mathbf{u}, \mathbf{x}, \varepsilon), \quad (23)$$

dependent on one parameter ε , which characterizes the object or external influence and takes the minimum value within the allowable range of control parameters \mathbf{u} . It is obvious that the optimal coefficients u_{i0} are functions of the parameter ε . The influence of the parameter ε on these coefficients is estimated by the derivative (sensitivity function) $\frac{du_i}{d\varepsilon}$.

It is known that the control parameters are determined using the necessary conditions for the minimum of Function (23)

$$\frac{\partial F}{\partial u_i} = \varphi[u_o(\varepsilon), \varepsilon] = 0 \quad i = \overline{1, n}. \quad (24)$$

Then, after differentiating the relations of (18), ε is obtained as follows:

$$\frac{\partial \varphi_i}{\partial \varepsilon} + \sum_{j=1}^n \frac{\partial \varphi_i}{\partial u_j} \cdot \frac{du_j}{d\varepsilon} = 0, \quad i = \overline{1, n}. \quad (25)$$

Expression (24) forms a system of linear inhomogeneous algebraic equations with respect to the derivative $\frac{du_j}{d\varepsilon}$. For a small $\Delta\varepsilon$ increase, the optimal coefficients can be determined as a result of linearization by the ratios

$$\Delta u_{i0} = \frac{du_j}{d\varepsilon} \Delta \varepsilon \quad (26)$$

In the case of several parameters of the object and disturbing effects, we have

$$\Delta u_{io} = \sum_{j=1}^m \frac{du_i}{d\varepsilon_j} \Delta \varepsilon_j$$

Let us now consider how the last problem is solved in the presence of constraints in the form of equalities:

$$g_j(u, \varepsilon) = 0, \quad j = \overline{1, p}. \quad (27)$$

It is known [27] that in this case, according to the Lagrange method, the auxiliary function

$$L = F + \sum_{j=1}^p \mu_j g_j \quad (28)$$

allows you to replace a constrained task with an unrestricted task. In Expression (22), the quantities μ_j are Lagrange factors. The necessary conditions for the presence of the minimum of the Function (20), taking into account the Conditions (22), take the form

$$\frac{\partial L}{\partial u_i} = 0, \quad i = \overline{1, n} \quad (29)$$

or

$$\frac{\partial F}{\partial u_i} + \sum_{j=1}^p \mu_j \frac{\partial g_j}{\partial u_i} = 0, \quad i = \overline{1, n}. \quad (30)$$

The variables u_i and μ_j can be found as a result of solving Equations (29) and (30). Derivatives of Expressions (29) and (30) by the parameters ε can be written as follows:

$$\left. \begin{aligned} \frac{\partial g_i}{\partial \varepsilon} + \sum_{j=1}^n \frac{\partial g_i}{\partial u_j} \cdot \frac{\partial u_j}{\partial \varepsilon} &= 0, \quad i = \overline{1, p}; \\ \frac{\partial \varphi_i}{\partial \varepsilon} + \sum_{j=1}^n \frac{\partial \varphi_i}{\partial u_j} \cdot \frac{\partial u_j}{\partial \varepsilon} + \sum_{j=1}^p \left[\frac{d\mu_j}{d\varepsilon} g'_{ji} + \mu_j \left(\frac{\partial g'_{ji}}{\partial \varepsilon} + \sum_{q=1}^n \frac{\partial g'_{ji}}{\partial u_q} \cdot \frac{\partial u_q}{\partial \varepsilon} \right) \right] &= 0, \quad i = \overline{1, p}, \end{aligned} \right\} \quad (31)$$

where

$$\varphi_i = \frac{\partial F}{\partial u_i}; \quad g'_{ji} = \frac{\partial g_j}{\partial u_i}$$

Expression (31) can be considered a system $(p + n)$ of linear algebraic equations with respect to derivatives $\frac{du_j}{d\varepsilon}$ and $\frac{d\mu_j}{d\varepsilon}$. The coefficients of these equations can be calculated or determined analytically by the known functions g_i and F . Derivatives characterizing the sensitivity of the optimal control parameters for RES in DT are the result of solving the considered algebraic system (31). In this case, derivatives can also be calculated by the parameter ε of Lagrange factors.

In Figure 10, an algorithm for solving the inverse sensitivity problem in an iterative way using criterion models for the assessment of DT RESs and improving the implementation of DT for RESs is shown.

Figure 10 shows the flowchart of the formation of the optimality region $\delta \mathbf{M}_u$. The algorithm is implemented as part of the software for sensitivity analysis of power generation RESs [27]. The software is compatible and works in a graphical and computing environment. Input data and analysis results are stored in a database (DB).

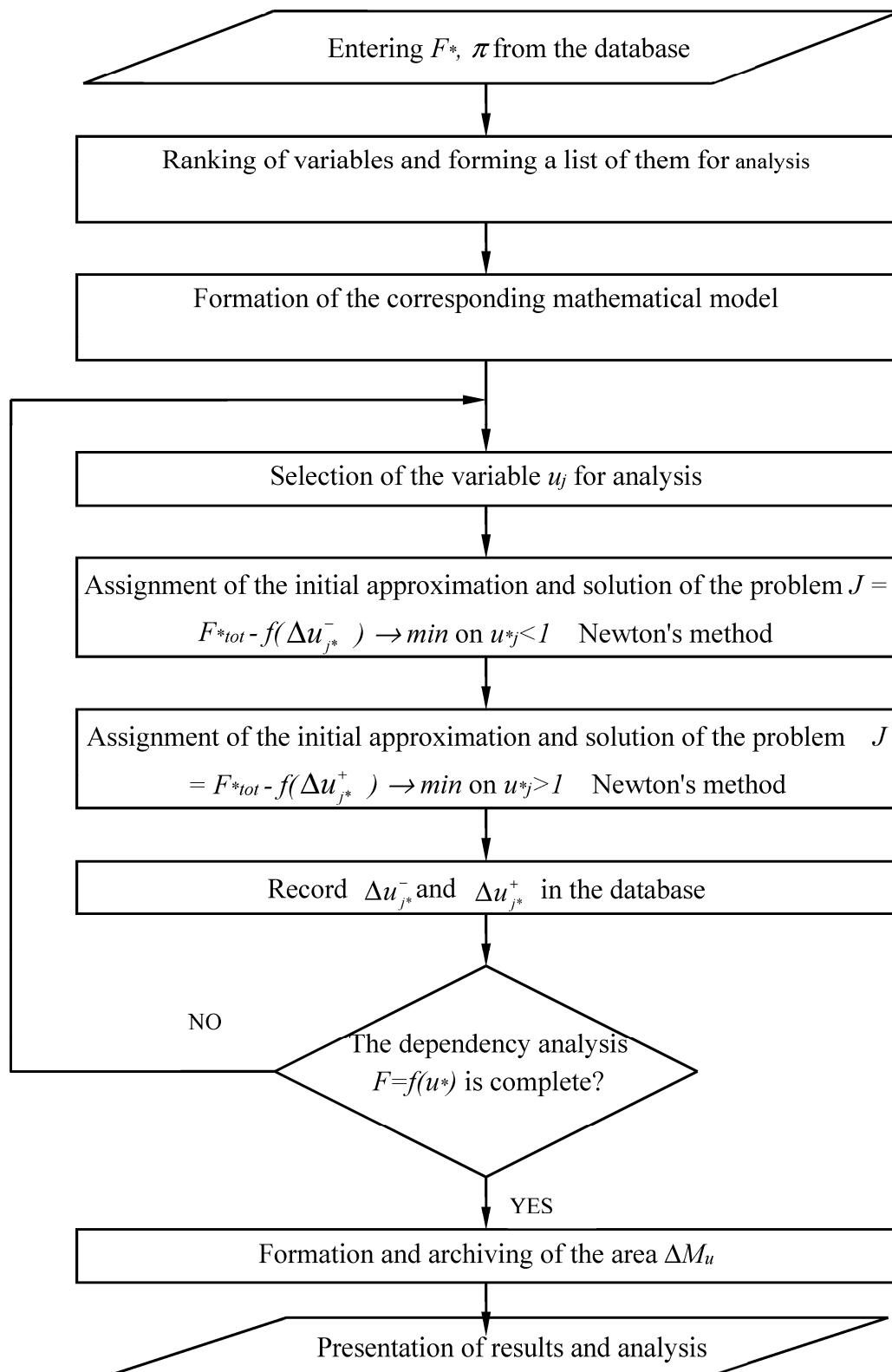


Figure 10. Algorithm for solving the inverse sensitivity problem in an iterative way using criterion models.

8. Investigation of Daily Electricity Generation RESs during the Year

Three different types of RESs were studied: photovoltaic power stations (PPSs) [32], wind power stations (WPSs) [31,34], and mini-hydropower stations (MHPs) [33,35]. Daily

electricity generation for each power station is shown in Figure 11: respectively, PPS (“Tsekynivska-2”–4–5, Ukraine) (see Figure 11a,b), MHPS (“Bodnarivska”, Ukraine) (see Figure 11c), WPS (Sokol, Poland). Consequently, in the case of RESs, such as for the WPS and PV power station, the output power generation cannot be arbitrarily adjusted [35]. The red graph shows the determined daily electricity generation, and the dark blue graph shows measured data (see Figure 11c). During 2019, real data were observed and kept about daily electricity generation by mini-HPP “Bodnarivska”. So, our predicted value for the annual electricity generation for 2019 was 1.472 GWh, but in reality, we had 1.322 GWh (Error is 11%). However, for forecasting, we take into account only meteorological factors and use the standard expression, but did not use dispatch control and technical condition equipment.

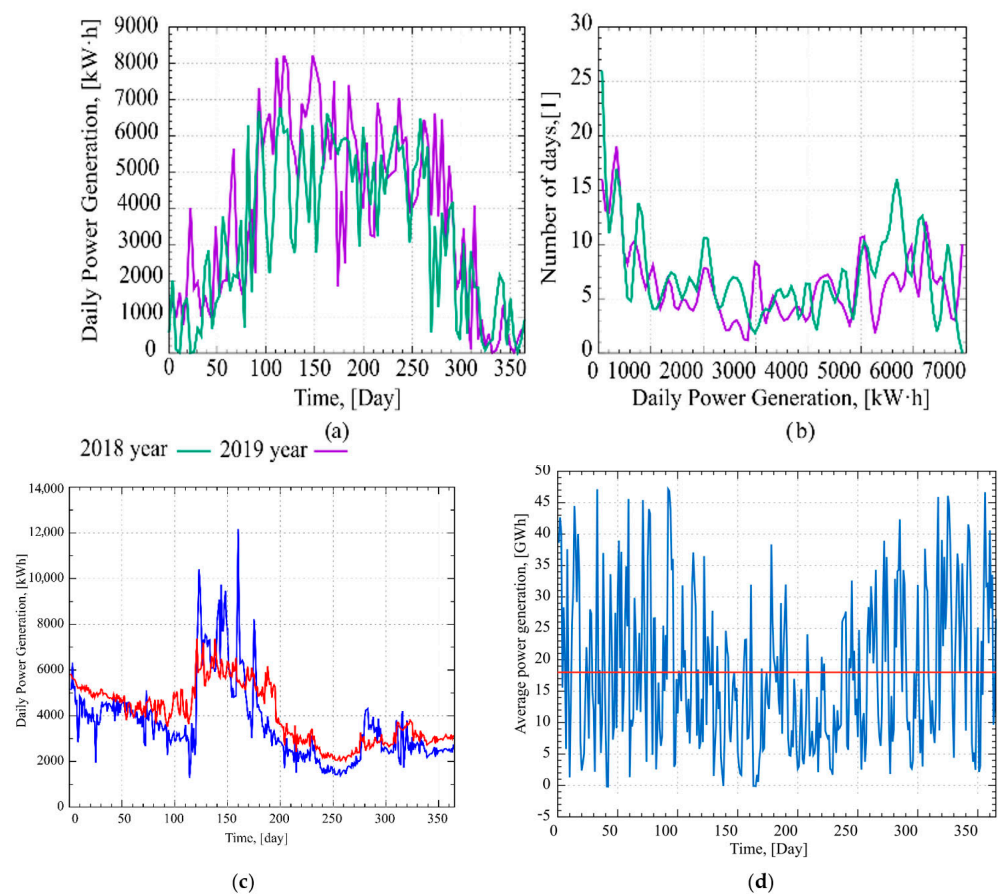


Figure 11. Daily electricity generation (2018–2019) by PPS “Tsekynivska-2”–4–5 (a) and distribution of number of days depending on value electricity generation (b) [32]; daily electricity generation by mini-HPP “Bodnarivska” during the 2019 year (c): red curve is calculated value and blue curve is real value [34]; and daily electricity generation of WPP during the 2019 year (d) [36].

The most significant difference between centralized power supply in the power grids and distributed power generation is the change in power flows in different directions of electricity and the structure of load and consumption charts. The balance structure usually depends strongly on the consumption schedule and its variability. In power systems that use large amounts of RESs but lack sufficient storage reserves, the composition of production units varies under the influence of many factors. These factors usually include meteorological conditions, as well as the topology of transmission and distribution lines to consumers. In particular, the structure of the equipment and lines can change significantly, which affects the entire balance reliability of the entire system. Therefore, it is important to assess the possibility of ensuring the balance reliability of RESs in electrical networks, taking into account their schedules of generation and consumption. However, obtained graphs in

Figure 9 show the instability of average daily electricity generation during the year. The processes of changing the daily and hourly electricity generation of RESs during the year, day, and hour depend on the influence of meteorological factors, electricity consumption schedules, parameters that characterize the technical condition of electrical equipment networks, and so on.

For assessment of the influence of meteorological factors on generation by RESs, the correlation–regression analysis can be applied. The main task of the correlation–regression analysis is to define and assess the most significant quantitative characteristics of particular relations between particular processes and phenomena. The Pearson, Spearman, and Kendall correlation coefficients are to be used for estimating this influence [37].

9. Correlation–Regression Analysis of RES Generation

The most common criterion for evaluating the closeness of the connection between variables is the Pearson correlation coefficient, which is given as follows:

$$r_{fW} = \frac{n \cdot \sum f_i \cdot W_i - (\sum f_i) \cdot (\sum W_i)}{\sqrt{(n \cdot \sum f_i^2 - (\sum f_i)^2) (n \cdot \sum W_i^2 - (\sum W_i)^2)}}, \quad (32)$$

where W_i is daily electricity generation and f_i is the meteorological factor. However, this has limited opportunities for usage due to the following requirements:

1. Comparative values should be on an interval or relative scale (quantitative and continuous);
2. At least one of the values (and preferably both) should have a normal distribution (because the calculation of this ratio is a parametric estimation method relationship sign);
3. The relationship between variables is linear;
4. Homoscedasticity;
5. Quite a large sample size of at least 25 observations.

Thus, before deciding to apply the Pearson correlation coefficient, we need to know the data type and distribution of the studied variables, and if this is unknown, then it is necessary to check the distribution of both variables in the sample. Additionally, there is the need to build the scattergram in order to ensure that the relationship between variables is linear, and to check the condition of homoscedasticity. If this condition is met, the data scatter of the variable W_i is approximately the same for all values of the variable f_i . If the variability of the variable W_i varies depending on the value of the variable f_i (the scattergram looks like a triangle, trapezoid, etc.), then the Pearson correlation coefficient does not properly reflect the relationships between variables. Checking the normality of the data distribution and analysis of the scattergram allowed us to conclude that other criteria could be applied, such as Spearman’s rank coefficient [32,37].

Correlation analysis of the basic variables was applied. The use of ordinal variables allowed us to order statically described objects according to the degree of appearance of particular features. The usage of ordinal variables is necessary when the scale of direct quantitative measurement of the object is unknown or just in the basic conventional sense. Since the RES electricity generation and meteorological parameters are always tied to the timeline, this allowed us to rank them according to the ordinal variables (time—year, month, day, hour, and minute). This fact is especially important if taking into account the problem of power balancing in today’s conditions of operating the electric power system.

Thus, in contrast to classical statistical analysis of the k_{th} ($k = 0, 1, 2, \dots, p$) quantitative, when the characteristic $x(k)$ is the result of real measurement or observation of physical objects, every statistical investigation matches one of several physical scales represented through numerical characteristic $x(k)$. In this case, the result of measuring the ordinal variable is a direct mapping to each feature of the studied objects. This is represented with some conditional numerical labels, and this representation determines the real position of this subject in the queue of all of the n studied objects, and these objects are ordered to

reduce the degree of manifestation like the k th test feature. This situation is called the rank of the i th object by the k th sign.

The process of ordering these objects P_1, P_2, \dots, P_n is performed using expert information, meaning involvement or formalization. This could be expressed by repositioning from an initial series of some auxiliary quantitative observations to the corresponding variation set. Typical measurement $p + 1$ of the ordinal variables n of the studied objects P_1, P_2, \dots, P_n , makes a table of initial data and indexes. Any item from the table specifies a rank that occupies a specific position in the range of all statistically examined objects. These elements are sorted to reduce the degree of manifestation of the k th test feature. This feature is represented as a variable. In this meaning, the rank correlation is a statistical relationship between those ordinal variables. This means that the relationship is analyzed on the basis of the initial statistics. All inputs are represented by the indexes of n objects understood on different grounds. Assessing the consistency or relationship between the structure of the indexing describes investigated objects in the sign $x^{(k)}$ and the ordering of the same objects by another sign $x^{(j)}$ (Table 2) [35,37–39].

Table 2. The relationship between the ordering of the investigated objects by the sign $x^{(k)}$ and the ordering of the same objects by another sign $x^{(j)}$.

Ordinal Number of the Object	Ordinal Number of the Investigated Variable (“Property”)							
	0	1	2	3	...	k	...	p
1	$x_1^{(0)}$	$x_1^{(1)}$	$x_1^{(2)}$	$x_1^{(3)}$...	$x_1^{(k)}$...	$x_1^{(p)}$
2	$x_2^{(0)}$	$x_2^{(1)}$	$x_2^{(2)}$	$x_2^{(3)}$...	$x_2^{(k)}$...	$x_2^{(p)}$
⋮
i	$x_i^{(0)}$	$x_i^{(1)}$	$x_i^{(2)}$	$x_i^{(3)}$...	$x_i^{(k)}$...	$x_i^{(p)}$
⋮
n	$x_n^{(0)}$	$x_n^{(1)}$	$x_n^{(2)}$	$x_n^{(3)}$...	$x_n^{(k)}$...	$x_n^{(p)}$

To determine the degree of connection between the rankings $X^{(k)} = (x_1^{(k)}, x_2^{(k)}, \dots, x_n^{(k)})^T$ and $X^{(j)} = (x_1^{(j)}, x_2^{(j)}, \dots, x_n^{(j)})^T$, Spearman’s rank correlation coefficient is used:

$$\hat{r}_{kj}^{(s)} = 1 - \frac{6}{n^3 - n} \sum_{i=1}^n (x_i^{(k)} - x_i^{(j)})^2 \tag{33}$$

For equaling ranks $x_i^{(k)} = x_i^{(j)}$ for all $i = 1, 2, \dots, n$ is $\hat{r}_{kj}^{(s)} = 1$, and for opposite $x_i^{(k)} = n - x_i^{(j)} + 1$ for $i = 1, 2, \dots, n$ is $\hat{r}_{kj}^{(s)} = -1$. In all other cases, $|\hat{r}_{kj}^{(s)}| < 1$ [40–42].

Another widely used characteristic of the closeness of the statistical relationship between the two rankings is the Kendall rank correlation coefficient, which is determined by the ratio

$$\hat{r}_{kj}^{(K)} = 1 - \frac{4\nu(X^{(k)}, X^{(j)})}{n(n - 1)}, \tag{34}$$

where $\nu(X^{(k)}, X^{(j)})$ is the minimum number of exchanges of adjacent elements of the sequence $X^{(j)}$ necessary to bring it to order $X^{(k)}$. Obviously, the value $\nu(X^{(k)}, X^{(j)})$ is symmetric with respect to its arguments, so the number of exchanges is minimal for the sequence $X^{(k)}$, necessary to bring to form $X^{(j)}$. With matching rankings $X^{(k)}$ and $X^{(j)}$ $\hat{r}_{kj}^{(K)} = 1$ ($\nu(X^{(k)}, X^{(j)}) = 0$), and at opposite

$$x_i^{(k)} = n - x_i^{(j)} + 1, i = 1, 2, \dots, n,$$

so

$$v(X^{(k)}, X^{(j)}) = \frac{1}{2}n(n-1)\hat{r}_{kj}^{(K)} = -1.$$

In all other cases,

$$|\hat{r}_{kj}^{(K)}| < 1.$$

The Kendall coefficient is defined on the basis of ratios of the type “more or less”, the validity of which is established when constructing scales. A pair of objects are selected, and their ranks are compared on one basis and on another. If, on the first sign, the ranks form a direct order (the order of a natural series), then the pair is assigned +1; if the reverse is true, then −1.

For the selected pair, the corresponding plus–minus units (on the basis of X and on the basis of Y) are multiplied. The result is +1 if the ranks of the pair of both traits are in the same sequence, and −1 if in reverse.

The Kendall coefficient has some advantages over the Spearman coefficient; namely, when you need to thoroughly investigate the statistical features of the data and the dynamics of changes, this coefficient is more precise. The coefficients for data on meteorological factors were obtained in Power Project Data Sets (see Figure 12) [43].

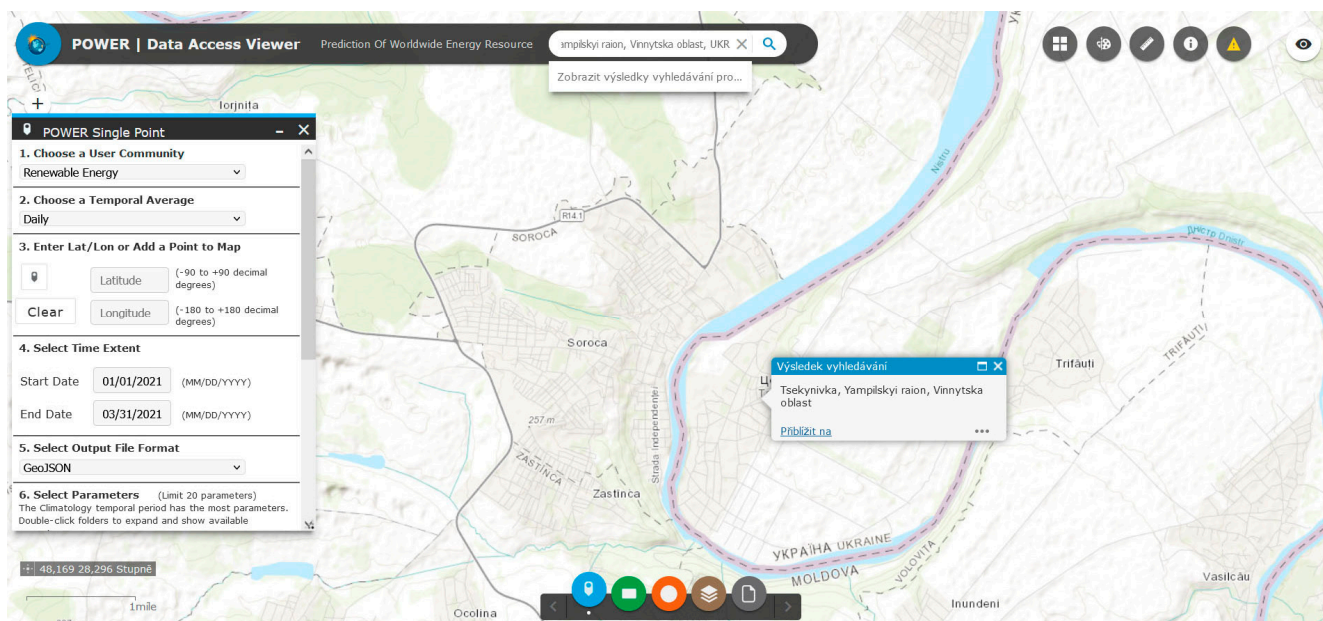


Figure 12. Formation of a meteorological database using NASA Prediction of Worldwide Energy Resources POWER Release-8 [30].

To obtain data about meteorological factors, the free NASA resource Power Project Data Sets was used. The flowchart shows how to obtain meteorological data step-by-step (see Figure 12).

The Pearson, Spearman, and Kendall correlation coefficients were used to comprehend and optimize the meteorological factors that influence the electricity generation of different kinds of RESs.

LabView software was used to estimate and compose Pearson, Spearman, and Kendall rank correlation coefficients.

Results are noted in Table 3 and Figure 13.

Table 3. The results of determining the Kendall, Spearman, and Pearson correlation coefficients of electricity generation.

Name of Influential Factors	Description	Spearman's Rank correlation Coefficient Mini—HPS 2019	Kendall's rank Correlation Coefficient Mini—HP 2019	Pearsons Rank Correlation Coefficient Mini—HPS 2019	Spearman's Rank Correlation Coefficient PPS 2018	Kendall's Rank Correlation Coefficient Mini—PPS 2018	Pearsons Rank Correlation Coefficient PPS 2018	Spearman's Rank Correlation Coefficient PPS 2019	Kendall's Rank Correlation Coefficient PPS 2019	Pearsons Rank Correlation Coefficient PPS 2019	Spearman's Rank Correlation Coefficient Mini—WPS 2019	Kendall's Rank Correlation Coefficient Mini—WPS 2019	Pearsons Rank Correlation Coefficient Mini—WPS 2019
PRECTOT	Precipitation	0.23	0.26	0.159	−0.411	−0.286	−0.230	−0.371	−0.254	−0.16	0.05	0.008	0.07
QV2M	Specific Humidity at 2 m	−0.03	0.036	−0.113	0.659	0.539	0.669	0.476	0.389	0.478	−0.16	−0.2	−0.19
RH2M	Relative Humidity at 2 m	0.35	0.27	0.236	−0.747	−0.530	−0.739	−0.764	−0.550	−0.76	0.145	0.23	0.22
PS	Surface Pressure	−0.14	−0.14	−0.094	−0.036	−0.020	−0.049	0.099	0.067	0.096	−0.08	−0.19	−0.12
T2M RANGE	Temperature Range at 2 m	−0.21	−0.15	−0.143	0.729	0.524	0.735	0.705	0.507	0.710	−0.13	−0.2	−0.19
TS	Earth Skin Temperature	−0.18	−0.002	−0.132	0.703	0.492	0.729	0.716	0.518	0.719	−0.18	−0.26	−0.26
T2MDEW	Dew/Frost Point at 2 m	−0.04	0.12	−0.048	0.622	0.418	0.637	0.561	0.395	0.564	−0.16	−0.27	−0.24
T2MWET	Wet Bulb Temperature at 2 m	−0.04	0.12	−0.047	0.621	0.417	0.637	0.560	0.394	0.563	−0.16	−0.23	−0.24
T2M_MAX	MaxTemperature at 2 m	−0.2	−0.03	−0.141	0.749	0.534	0.772	0.746	0.550	0.751	−0.18	−0.27	−0.26
T2M_MIN	Minimum Temperature at 2 m	−0.15	0.02	−0.118	0.638	0.432	0.656	0.630	0.448	0.636	−0.17	−0.26	−0.25
T2M	Temperature at 2 Meters	−0.16	0.008	−0.123	0.703	0.491	0.728	0.713	0.517	0.717	−0.17	−0.26	−0.26
WS50M_RANGE	Wind Speed Range at 50 m	0.06	0.08	0.043	0.109	0.074	0.064	0.042	0.028	0.027	0.02	0.04	0.027
WS10M_RANGE	Wind Speed Range at 10 m	0.09	0.07	0.06	−0.061	−0.040	−0.100	−0.027	−0.020	−0.03	0.23	0.29	0.342
WS50M_MIN	Minimum Wind Speed at 50 m	−0.05	−0.096	−0.024	−0.183	−0.120	−0.201	−0.190	−0.125	−0.198	0.45	0.67	0.62
WS10M_MIN	Minimum Wind Speed at 10 m	−0.09	−0.13	−0.054	−0.170	−0.112	−0.199	−0.199	−0.134	−0.224	0.42	0.61	0.6
WS50M_MAX	Maximum Wind Speed at 50 m	<−0.001	−0.03	0.007	−0.100	−0.065	−0.140	−0.158	−0.106	−0.15	0.51	0.61	0.67
WS10M_MAX	Maximum Wind Speed at 10 m	<−0.001	−0.03	0.006	−0.183	−0.121	−0.202	−0.173	−0.116	−0.15	0.49	0.62	0.67
WS50M	Wind Speed at 50 m	−0.02	−0.07	−0.005	−0.189	−0.125	−0.189	−0.189	−0.126	−0.18	0.55	0.7	0.71
WS10M	Wind Speed at 10 m	−0.01	−0.06	−0.003	−0.209	−0.136	−0.224	−0.227	−0.152	−0.22	0.53	0.68	0.7
KT	Insolation Clearness Index	−0.02	0.002	−0.019	0.840	0.653	0.838	0.791	0.599	0.798	−0.09	−0.16	−0.14
ALLSKY_SFC_SW_DWN	All Sky Insolation Incident on a Horizontal Surface	0.08	0.18	0.04	0.916	0.748	0.914	0.894	0.731	0.892	−0.18	−0.27	−0.27
ALLSKY_SFC_LW_DWN	Thermal Infrared Radiative Flux	−0.07	0.08	−0.06	0.408	0.252	0.385	0.424	0.288	0.413	−0.16	−0.25	−0.24

with the maximum possible accuracy by comparing our own photo documentation with the provided drawings. Any deviations, however, do not have a significant effect on the functionality and accuracy of the created model. So it can provide problems during the process of creating DT RESs.

The actual model is created with two variants. One model is clearer, but does not include remote shading objects that can affect the operation of the PV system located on the building (e.g., other big buildings). The second variant contains the same elements but is incorporated into the map base and also contains models of shading objects that were selected based on the shading analysis.

The model of the unit itself is made up of several separate objects that are graphically described (building low, building high, and so on). Individual mounting surfaces are supplemented with details that affect the use of the surface or the creation of shadows (blinds, vents, etc.). Mounting surfaces also contain individual protective zones (lightning conductors, gas, edges of buildings, etc.). If part of the mounting surface is covered by an adjacent object, this area is filled with a forbidden area to allow the use of automatic tools for creating PV systems. Individual mounting surfaces and important functional elements are also mnemonically described in the model for easy orientation. For a better overview of the overall situation, the individual elements are textured using textures obtained from the captured photos. The created model of the industrial building is shown in Figure 12, and the overall situation is shown in Figures 14 and 15.

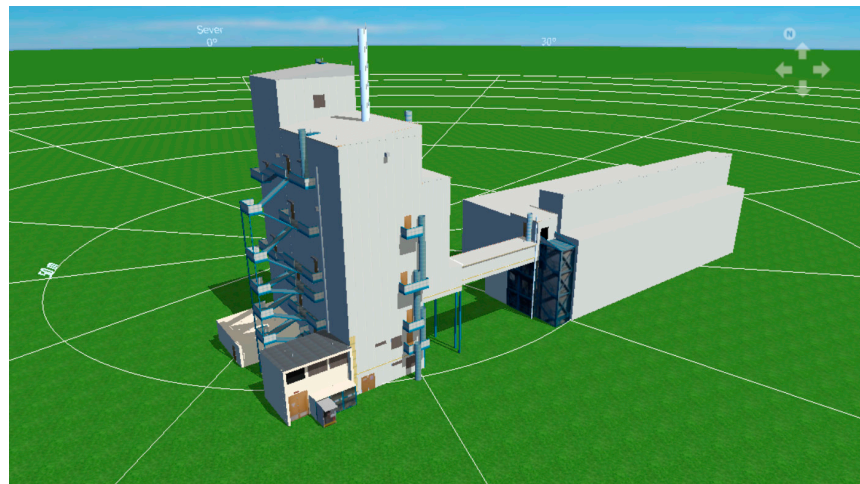


Figure 14. Three-dimensional model of the unit and adjacent objects.



Figure 15. Three-dimensional model of the unit area, including shading objects.

12. Feasibility Study of the PV Power Plant in the Current State of the Building

So, the created variants represent three different solutions with different degrees of utilization of building surfaces and different complexity of solutions. The complexity and complexity of the mounting surfaces offer a lot of room for the variability of individual solutions. Due to aesthetics and, in particular, trouble-free functionality, different types of panels are not used in individual variants (with one exception). Modern 500 W monocrystalline silicon half-cut Longi LR5 HIIH 500M modules were used for the simulation. The use of smaller modules (200–300 W) could probably achieve even better use of individual surfaces, but due to the large variability of the shading density, the correct detection and limitation of these areas have a more significant effect on the functioning of the system. Certain inaccuracies in the placement of individual details on the assembly surfaces also play their role (it cannot be determined unequivocally from the documentation). To detect these effects, panels rotated by 90° were used in some variants. The resulting deviation varies at most in percentage units. All variants are designed with maximum simplicity in mind. The modules and inverters used are currently commonly available on the market. Only general economic parameters are used in the simulations, which do not guarantee the absolute correctness of the results. Individual variants, however, can be compared relatively among themselves.

12.1. Variant 01

The system is supplemented by thin-film CIS panels 140 W on the northern walls. Emphasis is placed on the maximum use of individual surfaces and the maximization of installed power. Utilization of northern areas increases production by about 10% over Variant 01, but overall utilization and internal rate of return are somewhat worse. From the simulations, it is again clear that some surfaces have up to 50% losses due to shading and are, therefore, not suitable for real use (Figure 14).

Installed capacity: 258 kWp (784 modules)–27 areas
Estimated annual production: 137,320 kWh
Specific annual yield: 530.09 kWh/kWp
Utilization rate: 73.1%
Internal rate of return: 6.23%

12.2. Variant 02

This is an addition to variant 04 with better use of low and shielded surfaces using thin-layer CIS panels. Surfaces are also used where panels can be damaged due to handling in adjacent areas (scale, dump under the conveyor...). This variant offers by far the greatest utilization of area, but the worst degree of utilization and internal rate of return.

Installed capacity: 269 kWp (866 modules)–27 areas
Estimated annual production: 139,171 kWh
Specific annual yield: 514.24 kWh/kWp
Utilization rate: 72.2%
Internal rate of return: 6.03%

12.3. Variant 03

Only vertical panels are used on the east, south, and west walls and sloping structures on the roofs. The emphasis is not on the maximum use of individual surfaces and maximizing the installed power, but on the efficiency of the entire system. Only surfaces with a maximum degree of shading of up to 5% are used. This rule guarantees the uniformity of the efficiency of individual strings and better use of the installed panels (Figures 16–18).

Installed power: 115 kWp (231 modules)–13 areas
Estimated annual production: 81,839 kWh
Specific annual yield: 706.12 kWh/kWp
Utilization rate: 86.3%
Internal rate of return: 8.39%



Figure 16. Simulation of variant 01.

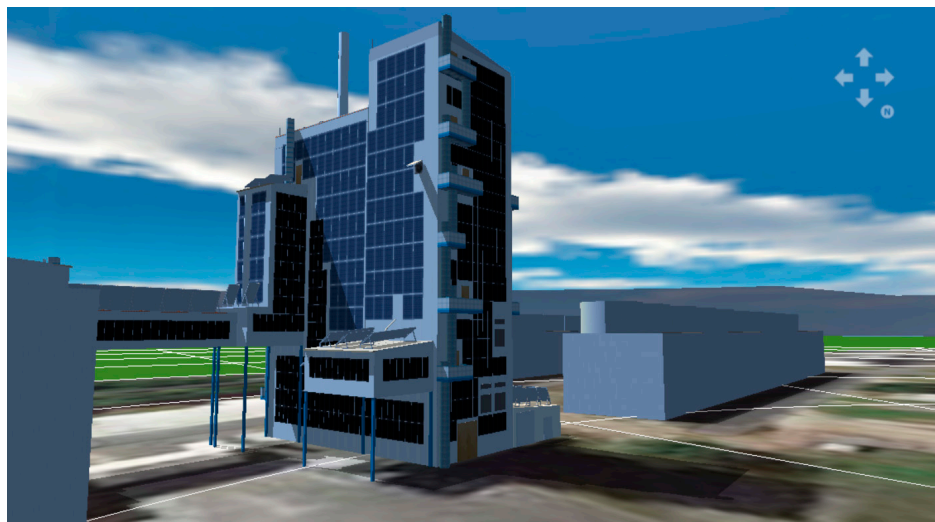


Figure 17. Simulation of variant 02.



Figure 18. Simulation of variant 03.

13. Discussion of the Case Study

Evaluation of the usability of individual variants for covering their own consumption was studied. All of the listed variants 01–03 can be used without problems to cover their own consumption, which is characterized by the delivered monthly values of electricity consumption. Considering the amount of their current own consumption (1,446,670 kWh was accepted) and the expected production of electricity from the PV system (approx. 70,000–120,000 kWh), it can be assumed that all the energy produced is consumed during normal operation of the calcination unit. Due to the nature of the operation, the consumption can be considered practically constant during the entire 24 h. From this point of view, there is no significant difference between the individual variants.

14. Plan for the Future

Summarizing the above, the objectives of the study conducted in this work were formulated in this paragraph. Their essence is as follows:

- To explore the possibilities and determine the optimal ways to use existing methods and tools of similarity theory and modeling and develop new ones in relation to the sensitivity problems of optimal solutions for DT RESs;
- To develop mathematical models for DT RESs that allow us to more effectively solve the problems of the sensitivity analysis of optimal solutions for controlling the conditions of dynamic systems;
- To develop a method for assessing the criterion method of sensitivity of the mathematical model of optimal control of system conditions for DT RESs with eigenvalues, in particular, the assessment of the sensitivity of similarity criteria;
- To develop an algorithm for DT RESs and a program for the distribution of the area of insensitivity (optimality) of the criterion of optimality between the parameters of the optimized system, in which the discrepancy between the current and optimal conditions is characterized by large losses;
- To develop methods, algorithms, and programs for forming the laws of optimal control for RESs, taking into account the sensitivity and the example of optimizing the normal conditions of the EPS with RESs to make sure of their efficiency and effectiveness.

15. Conclusions

The obtained results can be used for the advancement of the research field as scientific substantiation of DTs and developed calculation methods for the design of power supply for objects and structures of various purposes using the heat of the environment and other renewable sources with redundancy for energy accumulation and consumption for solar energy, wind, and mini-hydropower plants. Another advancement is the development of practical recommendations for the construction of such energy systems that take into account meteorological available data. The developed models will offer the possibility of adaptation to different climatic zones and weather conditions and their application in isolated objects or integrated combined energy systems. Developed recommendations can be used for the renovation of the Power system of Ukraine and for the design of industry objects and shelters after the war following decarbonization, decentralization, and digitalization policy requirements by the EU. Observed research can help create the DT of a particular object (for example, a shelter) with RESs (design and simulate power and heat supply and consumption of shelters based on RESs using DT technology).

Author Contributions: Conceptualization, M.B. and O.R.; methodology, O.R. and M.B.; validation, M.B. and O.R.; formal analysis, M.B. and O.R.; investigation, M.B. and O.R.; resources, M.B. and O.R.; writing—original draft preparation, M.B. and O.R.; writing—review and editing, M.B. and O.R. All authors have read and agreed to the published version of the manuscript.

Funding: This study was supported by projects 23-PKVV-011 and MSCA4Ukraine ID number 1233365.

Data Availability Statement: The data presented in this study are available on request from the corresponding author.

Conflicts of Interest: The authors declare no conflict of interest. The funders had no role in the design of the study; in the collection, analyses, or interpretation of data; in the writing of the manuscript, or in the decision to publish the results.

References

1. Oh, S.; Shin, H.; Cho, H.; Lee, B. Transient Impact Analysis of High Renewable Energy Sources Penetration According to the Future Korean Power Grid Scenario. *Sustainability* **2018**, *10*, 4140. [CrossRef]
2. Nazir, M.S.; Ali, Z.M.; Bilal, M.; Sohail, H.M.; Iqbal, H.M. Environmental impacts and risk factors of renewable energy paradigm—a review. *Environ. Sci. Pollut. Res.* **2020**, *27*, 33516–33526. [CrossRef] [PubMed]
3. Bajaj, M.; Singh, A.K. Grid integrated renewable DG systems: A review of power quality challenges and state-of-the-art mitigation techniques. *Int. J. Energy Res.* **2019**, *44*, 26–69. [CrossRef]
4. International Renewable Energy Agency. *Renewable Energy Targets in 2022: A Guide to Design*, International Renewable Energy Agency; IRENA: Abu Dhabi, United Arab Emirates, 2022; ISBN 978-92-9260-480-6.
5. Available online: <https://www.irena.org/Digital-Report/World-Energy-Transitions-Outlook-2022#page-1> (accessed on 1 May 2023).
6. Available online: https://www.irena.org/-/media/Files/IRENA/Agency/Statistics/Statistical_Profiles/Europe/Ukraine_Europe_RE_SP.pdf (accessed on 1 May 2023).
7. Brosinsky, C.; Westermann, D.; Krebs, R. Recent and prospective developments in power system control centers: Adapting the digital twin technology for application in power system control centers. In Proceedings of the 2018 IEEE International Energy Conference (ENERGYCON), Limassol, Cyprus, 3–7 June 2018; pp. 1–6.
8. Brosinsky, C.; Westermann, D.; Krebs, R. Digital Twins: A Survey on Enabling Technologies, Challenges, Trends and Future Prospects. *IEEE Commun. Surv. Tutor.* **2022**, *24*, 2255–2291. [CrossRef]
9. Krummacker, D.; Reichardt, M.; Fischer, C.; Schotten, H.D. Digital Twin Development: Mathematical Modeling. In Proceedings of the 2023 IEEE 6th International Conference on Industrial Cyber-Physical Systems (ICPS), Wuhan, China, 8–11 May 2023; pp. 1–8. [CrossRef]
10. ENTSO. Technology Digital Twins. 2022. Available online: <https://www.entsoe.eu/news/2022/12/20/entso-e-and-dso-entity-signed-today-the-declaration-of-intent-for-developing-a-digital-twin-of-the-european-electricity-grid/> (accessed on 1 May 2023).
11. ENTSOE. Proposal Digitalization of Energy Action Plan. 2022. Available online: https://ee-public-nc-downloads.azureedge.net/strapi-test-assets/strapi-assets/2022_ENTSO_E_Market_report_Web_836ec0a601.pdf (accessed on 1 May 2023).
12. Nguyen, V.H.; Tran, Q.T.; Besanger, Y.; Jung, M.; Nguyen, T.L. Digital twin integrated power-hardware-in-the-loop for the assessment of distributed renewable energy resources. *Electr. Eng.* **2022**, *104*, 377–388. [CrossRef]
13. Digitalisation of the Energy System. Available online: <https://cordis.europa.eu/article/id/436700-digitalisation-of-the-energy-system> (accessed on 1 May 2023).
14. SO-DSO-Consumer Interface Architecture. Available online: <https://ec.europa.eu/inea/en/horizon-2020/projects/h2020-energy/grids-storage-energy-systems/interrface> (accessed on 1 May 2023).
15. New Technological Solutions to Make Renewable Energy More Reliable and Affordable (FLEXIGRID). Available online: <https://cordis.europa.eu/project/id/864048> (accessed on 1 May 2023).
16. Innovative Tools for the Digital Energy Market (TwinERGY). Available online: <https://www.twenergy.eu/twenergy-system> (accessed on 1 May 2023).
17. Increase Friendly Integration of Reliable PV Plants Considering Different Market segments. Available online: <https://cordis.europa.eu/project/id/952957> (accessed on 1 May 2023).
18. Brazier, R.; De Luca, E.; de Wit, P.; Eklund, H.; Gimeno, C.; Herbretau, S.; Zawadska, K. Smart Grid Key Performance Indicators: A DSO Perspective. Available online: https://cdn.eurelectric.org/media/5272/smart_grid_key_performance_indicators__a_dso_perspective-2021-030-0129-01-e-h-B85F16BF.pdf (accessed on 1 May 2023).
19. Lezhniuk, P.; Rubanenko, O.; Komar, V.; Sikorska, O. Sensitivity of the Model of the Process Making the Optimal Decision for Electric Power Systems in Relative Units. In Proceedings of the 2020 IEEE KhPI Week on Advanced Technology (KhPIWeek), Kharkiv, Ukraine, 5–10 October 2020; pp. 247–252. [CrossRef]
20. Čonka, Z.; Kolcun, M.; Morva, G. Impact of Renewable Energy Sources on Power System Stability. *Sci. J. Riga Tech. Univ.* **2014**, *32*, 29–34. [CrossRef]
21. Faraji, J.; Hashemi-Dezaki, H.; Ketabi, A. Multi-year load growth-based optimal planning of grid-connected microgrid considering long-term load demand forecasting: A case study of Tehran, Iran. *Sustain. Energy Technol. Assess.* **2020**, *42*, 100827. [CrossRef]
22. Faraji, J.; Ketabi, A.; Hashemi-Dezaki, H.; Shafie-Khah, M.; Catalao, J.P. Optimal day-ahead scheduling and operation of the prosumer by considering corrective actions based on very short-term load forecasting. *IEEE Access* **2020**, *8*, 83561–83582. [CrossRef]
23. Hashemi-Dezaki, H.; Hariri, A.M.; Hejazi, M.A. Impacts of load modeling on generalized analytical reliability assessment of smart grid under various penetration levels of wind/solar/non-renewable distributed generations. *Sustain. Energy Grids Netw.* **2019**, *20*, 100246. [CrossRef]

24. Lezhniuk, P.; Komar, V.; Kravchuk, S. Regimes Balancing in the Local Electric System with Renewable Sources of Electricity. In Proceedings of the 2019 IEEE 20th International Conference on Computational Problems of Electrical Engineering (CPEE 2019), Lviv-Slavske, Ukraine, 15–18 September 2019.
25. Gundebommu, S.L.; Rubanenko, O.; Cosovic, M. Determination of Normative Value Power Losses in Distribution power grids with Renewable Energy Sources using Criterion Method. In Proceedings of the 2020 19th International Symposium INFOTEH-JAHORINA, INFOTEH 2020, East Sarajevo, Bosnia and Herzegovina, 18–20 March 2020.
26. He, Y.; Li, F.; Wang, X.; Shen, S.; Zhu, K. Research on Instability of Distributed Renewable Energy Power Access to Distribution Network. In Proceedings of the 2019 IEEE 3rd Information Technology, Networking, Electronic and Automation Control Conference (ITNEC), Chengdu, China, 15–17 March 2019; pp. 38–41.
27. Lezhniuk, P.; Komar, V.; Rubanenko, O.; Ostra, N. The sensitivity of the process of optimal decisions making in electrical networks with renewable energy sources. *Prz. Elektrotechniczny* **2020**, *98*, 32–38. [CrossRef]
28. Burykin, O.B.; Malogulko, Y.V.; Tomashevskiy, Y.V.; Komada, P.; Orshubekov, N.A.; Kozhamberdiyeva, M.; Sagymbekova, A. Optimization of the functioning of the renewable energy sources in the local electrical systems. *J. Przegląd Elektrotechniczny* **2017**, *97*–103. [CrossRef]
29. Smolarz, A.; Lezhniuk, P.; Kudrya, S.; Komar, V.; Lysiak, V.; Hunko, I.; Amirgaliyeva, S.; Smailova, S.; Orazbekov, Z. Increasing Technical Efficiency of Renewable Energy Sources in Power Systems. *Energies* **2023**, *16*, 2828. [CrossRef]
30. Lezhniuk, P.; Komar, V.; Hunko, I.; Jarykbassov, D.; Tussupzhanova, D.; Yeraliyeva, B.; Katayev, N. Natural-Simulation Model of Photovoltaic Station Generation in Process of Electricity Balancing in Electrical Power System. *Inform. Autom. Pomiar. W Gospod. I Ochr. Sr.* **2022**, *12*, 40–45. [CrossRef]
31. Bělik, M. PV power stations—fire hotbeds and fire tolls. *Renew. Energy Power Qual. J.* **2019**, *17*, 229–234. [CrossRef]
32. Rubanenko, O.; Miroshnyk, O.; Shevchenko, S.; Yanovych, V.; Danylchenko, D.; Rubanenko, O. Distribution of Wind Power Generation Dependently of Meteorological Factors. In Proceedings of the 2020 IEEE KhPI Week on Advanced Technology (KhPIWeek), Kharkiv, Ukraine, 5–10 October 2020; pp. 472–477.
33. Rubanenko, O.; Yanovych, V. Analysis of instability generation of Photovoltaic power station. In Proceedings of the 2020 IEEE 7th International Conference on Energy Smart Systems, ESS, Kyiv, Ukraine, 12–14 May 2020; pp. 128–133.
34. Rubanenko, O.; Yanovych, V.; Miroshnyk, O.; Danylchenko, D. Hydroelectric Power Generation for Compensation Instability of Non-guaranteed Power Plants. In Proceedings of the 2020 IEEE 4th International Conference on Intelligent Energy and Power Systems (IEPS), Istanbul, Turkey, 7–11 September 2020; pp. 52–56.
35. Belik, M. Weather dependent mathematical model of photovoltaic panels. *Renew. Energy Power Qual. J.* **2017**. [CrossRef]
36. Gundebommu, S.L.; Hunko, I.; Rubanenko, O.; Kuchanskyy, V. Assessment of the Power Quality in Electric Networks with Wind Power Plants. In Proceedings of the 2020 IEEE 7th International Conference on Energy Smart Systems, ESS, Kyiv, Ukraine, 12–14 May 2020; pp. 190–194.
37. Belik, M. Emergency island grids with small hydro power stations. In Proceedings of the 10th International Scientific Symposium on Electrical Power Engineering, ELEKTROENERGETIKA 2019, Stará Lesná, Slovakia, 16–18 September 2019; pp. 116–121.
38. Belik, M.; Nohacova, L. Small hydro power plants operating as backup source in local island. In Proceedings of the 2019 20th International Scientific Conference on Electric Power Engineering, EPE, Kouty nad Desnou, Czech Republic, 15–17 May 2019.
39. Rao, A.C.S.; Somayajulu, D.; Banka, H. Modified correlation based technique in micro array data analysis for searching differentially expressed genes. In Proceedings of the 2012 1st International Conference on Recent Advances in Information Technology (RAIT), Dhanbad, India, 15–17 March 2012; pp. 526–530.
40. Khasawneh, A.; Qawaqzeh, M.; Miroshnyk, O.; Danylchenko, D.; Minakova, K.; Potryvai, A. Methodology for Accounting for the Influence of Dust Cover on the Performance of a Photovoltaic System for Matlab. In Proceedings of the 20th IEEE International Conference on Modern Electrical and Energy Systems, MEES 2021, Kremenchuk, Ukraine, 21–24 September 2021. [CrossRef]
41. Thirumalai, C.; Chandhini, S.A.; Vaishnavi, M. Analysing the concrete compressive strength using Pearson and Spearman. In Proceedings of the 2017 International conference of Electronics, Communication and Aerospace Technology (ICECA), Coimbatore, India, 20–22 April 2017; pp. 215–218.
42. Wang, H.; Lei, Z.; Zhang, X.; Zhou, B.; Peng, J. A review of deep learning for renewable energy forecast-ing. *Energy Convers. Manag.* **2019**, *198*, 111799. [CrossRef]
43. NASA Prediction of Worldwide Energy Resources. 2020. Available online: <https://power.larc.nasa.gov/> (accessed on 1 May 2023).

Disclaimer/Publisher’s Note: The statements, opinions and data contained in all publications are solely those of the individual author(s) and contributor(s) and not of MDPI and/or the editor(s). MDPI and/or the editor(s) disclaim responsibility for any injury to people or property resulting from any ideas, methods, instructions or products referred to in the content.